Journal of Power Sources 230 (2013) 155–160

Contents lists available at SciVerse ScienceDirect

Journal of Power Sources

journal homepage: www.elsevier.com/locate/jpowsour

Preparation and enhanced properties of dye-sensitized solar cells by surface plasmon resonance of Ag nanoparticles in nanocomposite photoanode

Kaimo Guo, Meiya Li*, Xiaoli Fang, Xiaolian Liu, Bobby Sebo, Yongdan Zhu, Zhongqiang Hu, Xingzhong Zhao

School of Physics and Technology, and the Key Laboratory of Artificial Micro/Nano Structures of Ministry of Education, Wuhan University, Wuhan 430072, PR China

HIGHLIGHTS

- Different amounts of Ag@TiO_2 core-shell nanoparticles were incorporated into DSSCs.
- The properties of the DSSC with 0.15 wt% Ag were significantly improved.
- The increase of J_{sc} may be attributed to enhanced dye light absorption.
- The enhanced light absorption was attributed to surface plasmon resonance of Ag.
- The increase of V_{oc} was attributed to the change of Fermi energy of Ag-TiO_2 system.

ARTICLE INFO

Article history:
Received 9 September 2012
Received in revised form
22 October 2012
Accepted 13 December 2012
Available online 27 December 2012

Keywords:
Titanium dioxide coated silver core–shell nanoparticles
Surface plasmon resonance
Absorption enhancement
Composite photoanode
Dye-sensitized solar cells

ABSTRACT

A series of TiO_2 photoanodes with differing amounts of Ag nanoparticles (NPs) on TiO_2 in core-shell form (Ag@TiO_2) are prepared and used to make a series of dye-sensitized solar cells (DSSCs). The influence of different amounts of Ag–NPs on the structure and performance of the DSSCs is investigated. Studies indicate that the short-circuit current density (J_{sc}), open-circuit voltage (V_{oc}), charge lifetime and dark current of DSSCs containing Ag–NPs are significantly improved. The best performance is achieved in the DSSCs with 0.15 wt% Ag–NPs additions, with the maximum J_{sc} of 10.19 mA cm^{-2}, highest V_{oc} of 698 mV and best photoelectric conversion efficiency of 5.33%, significantly superior to that of the DSSCs with pure TiO_2 photoanodes. The increase of J_{sc} is attributed to the enhanced dye light absorption in strength and spectral range due to the surface plasmon resonance of Ag–NPs in photoanode, while the increase of V_{oc} may be related to the more negative level of the quasi-Fermi energy of Ag–TiO_2 composite system resulting from the added Ag.

© 2012 Elsevier B.V. All rights reserved.

1. Introduction

Since dye-sensitized solar cells (DSSCs) were first proposed by O'Regan and Grätzel in 1991 [1], they have attracted considerable interest as an alternative to conventional silicon solar cells because of their low cost, simple fabrication on large-area flexible substrates, relatively high photon-to-current conversion efficiency [2] and potential economical advantages [3–5].

DSSCs typically consist of a nanocrystalline titanium dioxide photoanode film, dye molecules and redox electrolyte, and a counter-electrode in a sandwich structure. To obtain higher efficiencies DSSCs, TiO_2 photoanode films with various morphologies, such as nanoparticles (NPs) [6,7], ordered meso-structures [8], one-dimension structures (nanorods, nanowires, and nanotubes) [9–11] and various dopants [12–14], have been extensively explored. These efforts were made to improve the photocurrent, photovoltage, or both, to enhance DSSCs conversion efficiency. In addition, the dye is an important part of the DSSCs, playing a significant role in absorbing light, generating photo-stimulated carriers and injecting these carriers into the conduction band of TiO_2 network. Thus, the light absorption capability of the dye and how many carriers it stimulates directly affect carrier injection and DSSCs performance. Therefore, enhancing dye light absorption should be an effective way to increase the conversion efficiency.

* Corresponding author. Tel.: +86 27 68752481 3424; fax: +86 27 68752569.
E-mail address: myli@whu.edu.cn (M. Li).

0378-7753/$ – see front matter © 2012 Elsevier B.V. All rights reserved.
http://dx.doi.org/10.1016/j.jpowsour.2012.12.079

Recently, the surface plasmon resonance (SPR) of nanoparticles of noble metals such as gold, silver and copper has attracted much attention due to their unique electronic, optical and magnetic properties [15,16]. Ihara et al. have reported enhancement of the light absorption efficiency in dyes adsorbed on fine silver nanoparticles films [17]. However, there are few studies on the influence and mechanism of Ag–NPs on the performance of DSSCs. In this study, the effect of different amounts of Ag–NPs in Ag–TiO_2 nanocomposite photoanode was investigated.

2. Experiments

2.1. Synthesis of Ag@TiO_2 core–shell nanoparticles

Since electrolyte can permeate a porous TiO_2 film, bare Ag–NPs dispersed in the film may be easily etched by electrolyte, which may undermine or even eliminate the SPR effect. Hence, the use of Ag@TiO_2 core–shell nanoparticles (NPs) might be an effective way of protecting Ag from being eroded by electrolyte. Therefore, Ag@TiO_2 core–shell NPs sol was synthesized as follows. A mixture of 0.5 g Hydrazine (N_2H_4, SCRC-Ltd, Shanghai, CHN) (The SCRC-Ltd is the abbreviation of Sinopharm Chemical Reagent Co., Ltd.) and 0.036 g Hexadecyl trimethyl ammonium bromide (CTAB, SCRC-Ltd, Shanghai, CHN) was dissolved in 20 ml deionized water in a beaker and stirred vigorously at room temperature. 15 min later, 0.4 g silver nitrate ($AgNO_3$, SCRC-Ltd, Shanghai, CHN) was added in the solution, which was stirred until the color of the solution turned from transparent to light brown. Then, 0.028 g titanium tetraisopropoxide (TTIP, Acros Organics, New Jersey, USA) was added in solution, and stirring was continued for an additional 30 min to ensure completion of the reaction. A light brown solution containing Ag@TiO_2 core–shell NPs was then obtained. The solution was then centrifuged at 4000 rpm to remove CTAB and TTIP. The Ag@TiO_2 precipitate was redispersed in 5 ml of ethanol to form a light brown sol for further use.

2.2. Preparation Ag–TiO_2 composite photoanode

Ag–TiO_2 composite photoanode films were prepared by incorporating Ag–NPs in Ag@TiO_2 core–shell form into TiO_2 films. 2.5 g commercially available TiO_2 powder (P25, Evonik Degussa, Parsippany, NJ), 0.8 ml acetylacetone (surfactant, SCRC-Ltd, Shanghai, CHN) and 22.5 ml anhydrous ethanol (SCRC-Ltd, Shanghai, CHN) were mixed and ball milled in polytetrafluoroethylene (PTFE, SCRC-Ltd, Shanghai, CHN) container for 48 h. The glutinosity of the colloid of TiO_2 particles was adjusted by adding 4.5 ml of deionized water and 0.5 ml of emulsifier (Triton-100, SCRC-Ltd, Shanghai, CHN) into the colloid and milled for additional 1 h to obtain a milk-like pure P25 slurry. Different amounts of Ag@TiO_2 core–shell NPs were then added to this slurry, which was stirred for 24 h to form Ag–NP–doped P25 (Ag–P25) slurries with different mass ratios (Ag:P25 = 0.05, 0.10, 0.15, 0.20). These slurries were then made into films on the fluorine-doped SnO_2 conductive glass (FTO, sheet resistance 10–15 $\Omega\ sq^{-1}$, Asahi Glass, Japan) by doctor-blading with three-layer transparent tapes to control their thicknesses. These films were then dried under ambient conditions and annealed at 500 °C for 30 min to obtain an Ag–TiO_2 composite photoanode films of good uniformity and transmittance needed for cell assembly.

2.3. Device fabrication

The Ag–TiO_2 photoanodes prepared as above were sensitized by dipping them in the solution of cis-di(thiocyanato)-bis(2,2′-bipyridyl-4,4′-dicarboxylate) ruthenium(II) (N719, Solaronix, Switzerland) with a concentration of 500 μM in the mixture of anhydrous ethanol and tert-butyl alcohol (Acros Organics, New Jersey, USA) (volume ratio:1/1) at 60 °C overnight. The photoanodes were then washed with anhydrous ethanol to remove the excess dye molecules from the surface of the nanocrystalline TiO_2 to ensure that the porous film was covered with a monolayer of dye molecules. The fabrication process of typical sandwich-type DSSCs was carried out as follows. A platinized FTO counter-electrode was placed over a dye-sensitized photoanode, and then the two electrodes were clipped together to form an open cell. An electrolyte composed of 0.1 M 1-propy-3-methylimidazolium iodide (PMII, Acros Organics, New Jersey, USA), 0.05 M LiI (Acros Organics, New Jersey, USA), 0.1 M GNCS (Acros Organics, New Jersey, USA), 0.03 M I_2 (Yili chemicals, Beijing, CHN), 0.5 M 4-tert-butylpyridine (TBP, Acros Organics, New Jersey, USA) in acetonitrile (SCRC-Ltd, Shanghai, CHN)/propylene carbonate (PC) (SCRC-Ltd, Shanghai, CHN) (volume ratio:1/1) mixed solvent was injected into the open cell from the edges, and then the cell was tested immediately.

2.4. Characterizations

The surface morphologies of the Ag–TiO_2 photoanodes were observed by scanning electron microscopy (SEM, JEOL, 6700F, Japan). X-ray diffraction (XRD, D8 Advance, Bruker, Germany) was employed to characterize the crystalline structure of the Ag–TiO_2 films. The current density–voltage (J–V) characteristics of the cells were recorded under an irradiance of 100 mW cm^{-2} (AM 1.5 simulated illumination (Newport, 91192, Global)) calibrated by a Si photodiode. The effective irradiated area of each cell was kept as 0.25 cm^2 by using a light-tight metal mask for all samples. Electrochemical impedance spectra (EIS) were performed on a computer-controlled electrochemical workstation CHI660C (Shanghai, China) with a frequency range from 100 kHz to 0.1 Hz in the condition of open circuit. The UV–vis absorption spectra of the as-prepared sensitized samples were recorded on a UV–vis–NIR spectrophotometer (Cary 5000,Varian, USA).

3. Results and discussion

3.1. Microstructures of the photoanodes

Fig. 1 shows the XRD patterns of the Ag–TiO_2 films with different Ag–NPs content. The patterns showed that all films had

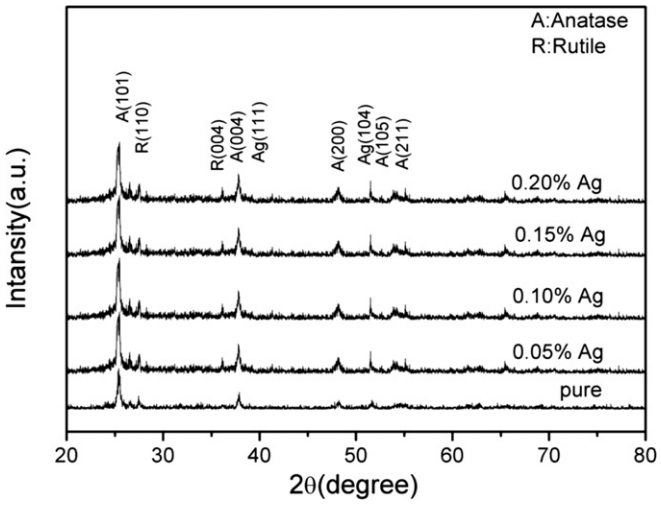

Fig. 1. X–ray diffraction patterns of different Ag–TiO_2 composite films.

good crystallinity. The characteristic peaks of (101), (200), (105) and (211) for anatase and (110) for rutile were observed in these patterns, indicating the coexistence of the anatase and rutile phases in the TiO_2. Besides these, characteristic peaks of Ag (111) and (104) were also observed in the patterns of the Ag–TiO_2 composite films, suggesting the stable existence of Ag–NPs in composite films. Meanwhile, the intensity of the anatase (101) peaks of the Ag–TiO_2 films increased with introduction of Ag–NPs, indicating that the higher crystallinity of the films compared to that of pure TiO_2. A rutile (004) peak was also observed in the patterns of Ag–TiO_2 films, suggesting a possible increase of the rutile phase in TiO_2. A certain amount of increase in rutile phase in TiO_2 would increase light scattering and absorption [18], which may enhance the short-circuit current of DSSCs.

3.2. Morphologies of Ag@TiO_2 NPs and Ag–TiO_2 films

Fig. 2 shows the TEM image of Ag@TiO_2 core–shell NPs dispersed in ethanol solution. Fig. 2(a) shows some black Ag spheres with a size of about 20 nm. While Fig. 2(b) shows the HRTEM image of an individual Ag@TiO_2 NP with the typical clear lattice fringes of crystalline Ag.

The SEM surface morphologies of the Ag–TiO_2 composite films are shown in Fig. 3(a)–(e). The SEM images show little difference between films with differing amounts of Ag–NPs, and all films showed compact morphologies and smooth surfaces.

The UV–vis spectra of (a) differing amounts of Ag–NPs dispersed in ethanol and (b) different Ag–TiO_2 photoanode films after sensitization are shown in Fig. 4. The amount of Ag–NPs dispersed in ethanol is the same as that in the composite films. Fig. 4(a) shows the strong absorption peaks of Ag–NPs with and without TiO_2 coating. The SPR originates from light (electromagnetic radiation) interacting with the free electrons of Ag–NPs, which results in the collective excitation oscillations that lead to strong enhancement of the local electromagnetic fields surrounding the nanoparticles. This enhanced electromagnetic field contributes to enhancing dye absorption. Compared to that of the bare Ag–NPs, the SPR absorption peak position of Ag@TiO_2 is shifted from 403 nm to 425 nm due to the change in the surrounding medium of Ag–NPs as a result of TiO_2 coating , which is consistent with an earlier study by Kelly et al. [18]. Moreover, the SPR peak intensity was enhanced with increasing Ag–NPs content, while no change in the peak position was observed.

Fig. 4(b) shows the UV–vis spectra of different Ag–TiO_2 composite photoanodes after sensitization. It can be seen that the intensity of SPR absorption peaks of the composite films increases with increasing Ag–NP content. Furthermore, the spectral absorption range was broadened with the long wavelength absorption edge shifting from 680 nm to the infrared region beyond 800 nm. This enhanced absorption and broadened spectrum-absorption range of the photoanodes were mainly attributed to the SPR of Ag–NPs, which interacted with the dye, enhancing dye absorption that resulted in more charge carrier generation. In this way, the J_{sc} and thus the photoelectric conversion efficiency of cells are significantly improved by the SPR effect [18,19].

3.3. Effect of SPR on the performance of DSSCs

To investigate the influence of SPR on the performance of cells, DSSCs based on TiO_2 and Ag–TiO_2 photoanodes were prepared. Fig. 5(a) shows the J–V curves of the DSSCs at AM 1.5 irradiation of 100 mW cm^{-2}. As shown in the J–V curves, the J_{sc} and V_{oc} both show significant regular variation with corresponding Ag–NP additions. The variation of J_{sc} and V_{oc} with Ag–NP loading are shown in Fig. 5(b). It is evident that the J_{sc} and V_{oc} both increased with the quantity of Ag–NP ranging from 0 to 0.15 wt%, and the maximum J_{sc} and V_{oc} were obtained at an optimized Ag–NPs content of 0.15 wt%. However, they began to decrease when the Ag–NPs content was more than 0.15 wt%. Since the value of the fill factor (FF) remained much the same, the conversion efficiency η showed a similar tendency of variation to that of the J_{sc} and V_{oc}, giving the maximum value of 5.33% with 0.15 wt% Ag–NP content. The performance parameters of the DSSCs are summarized in Table 1.

As can be seen in Table 1, DSSCs with 0.15 wt% Ag–NP addition gave a maximum J_{sc} of 10.19 mA cm^{-2}, 29.6% higher than the device with a pure TiO_2 photoanode. Obviously, the variation tendency of V_{oc} is similar to that of J_{sc}, which may be attributed to the effect of Ag–NPs additions. Since the FF of the cells remained around 0.67, the photoelectric conversion efficiency η of DSSCs was increased to 5.33% at the optimal Ag–NPs content, significantly superior to that of the pure TiO_2 cell. This shows the merits of introducing Ag–NPs into TiO_2 photoanodes. The increment of J_{sc} was attributed to the enhanced light absorption and broadened light absorption range of the dye (shown in Fig. 4) resulting from the SPR of Ag–NPs, which stimulated the dye to generate more charge carriers [20]. Furthermore, the Schottky barrier at the Ag/TiO_2 interface [21,22] will form electron–hole separation centers which would be beneficial in improving the movement of photo-generated electrons shuttling through the porous TiO_2 network, reducing recombination of electrons and holes, thus increasing J_{sc} [19]. The improvement of V_{oc} is associated with the electron storage capability of Ag–NPs.

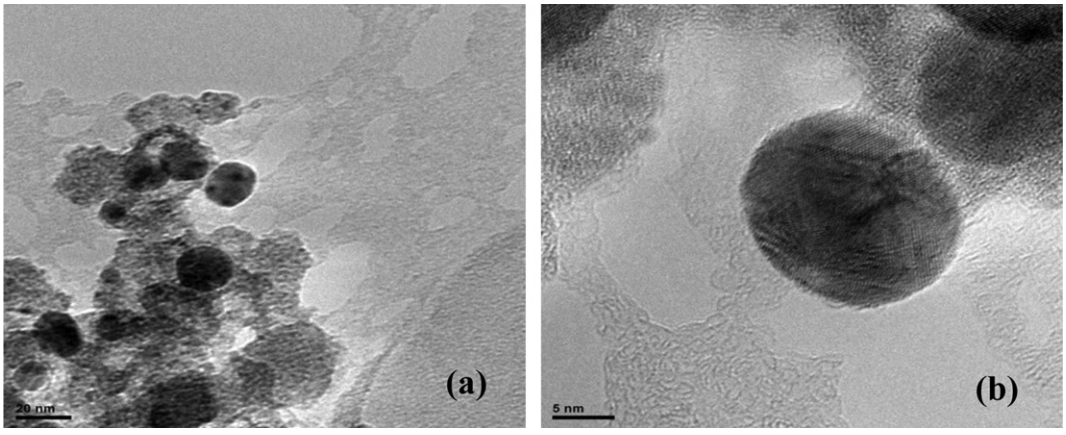

Fig. 2. (a) TEM and (b) HRTEM images of Ag@TiO_2 NPs in ethanol solution.

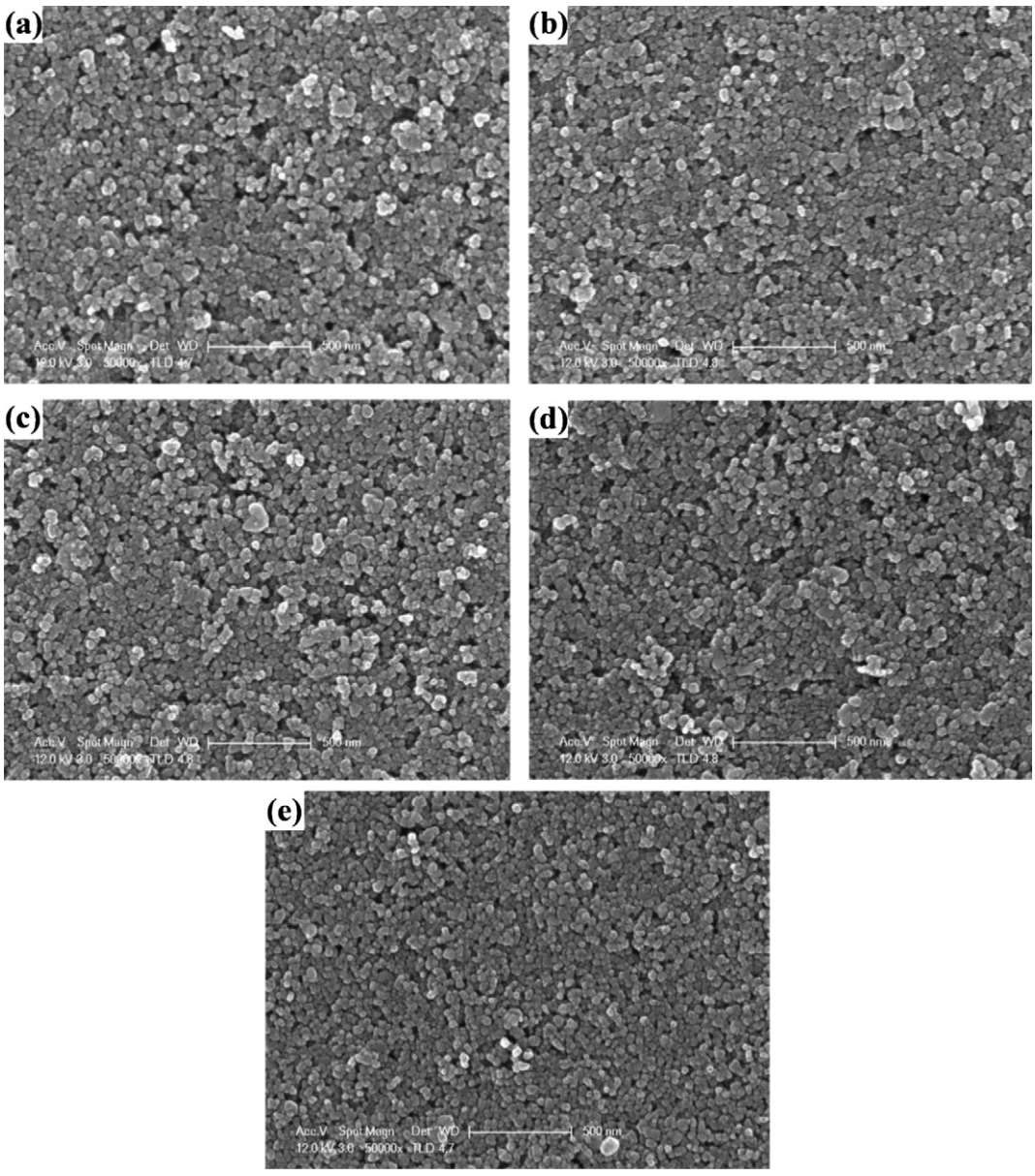

Fig. 3. SEM micrographs of surface morphologies for Ag–TiO_2 films containing (a) 0 wt%; (b) 0.05 wt%; (c) 0.10 wt%; (d) 0.15 wt%; (e) 0.20 wt% Ag after calcination at 500 °C.

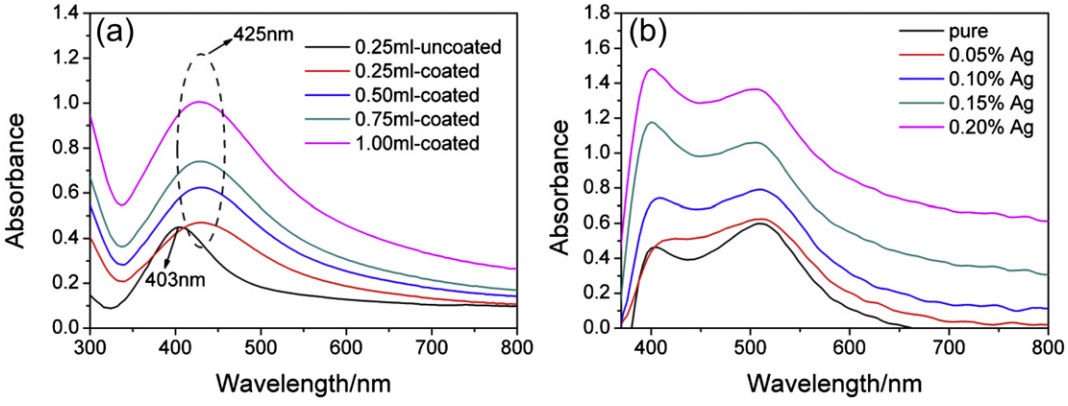

Fig. 4. UV–vis spectra of (a) different wt% Ag–NP dispersed in ethanol and (b) different Ag–TiO_2 composite films after sensitization.

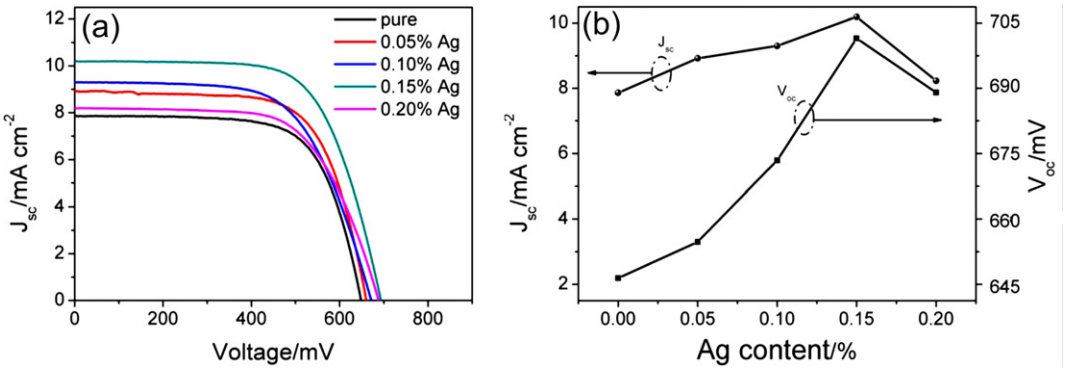

Fig. 5. (a) J–V curves of DSSCs with differing amounts of Ag–NP under AM 1.5 irradiation; light intensity 100 mW cm^{-2} and effective irradiation area 0.25 cm^2; (b) J_{sc} and V_{oc} as a function of Ag–NPs loading.

After rapid electron transfer from the conduction band of TiO_2 to Ag–NPs, followed by electron storage within them is clearly beneficial to the photoelectrochemical performance of the Ag–TiO_2 films. This makes the quasi-Fermi energy of the Ag–TiO_2 composite system shift to a more negative level compared to that of a pure TiO_2 photoanode, resulting in a higher V_{oc} [22]. However, the J_{sc} and V_{oc} both decreased when the Ag–NPs content reached 0.20 wt %. The reason for this may be explained as follows: Not all of the Ag–NPs in Ag@TiO_2 core–shell NP sol were entirely coated by TiO_2 to form the core–shell structure. Therefore, some of the bare Ag–NPs in the Ag–TiO_2 network structure may be eroded by electrolyte and oxidized to Ag^+ ions [23]. The latter act as a recombination center, reducing the number of charge carrier, thus resulting in a decrease in J_{sc} and V_{oc}. In addition, Ag–NPs (over 0.15 wt%) incorporated into the TiO_2 films might result in a reduced effective surface area of TiO_2 in contact with dye molecules. As a consequence, the recombination probability between electrons and holes may increase, so J_{sc} would decrease. In addition, higher concentrations of Ag–NPs may cluster to form larger Ag–NP groups with lower electron storage capability, reducing V_{oc} [22].

To investigate the charge transfer property of DSSCs, electrochemical impedance spectra (EIS) were obtained (Fig. 6). The Nyquist diagram features of two semicircles labeled as Z_1 and Z_2 were observed in the EIS spectra. From left to right, Z_1 represents the complex impedance of charge transfer at the TiO_2/conduction layer or Pt/electrolyte interfaces and Z_2 is associated with the TiO_2/dye/electrolyte interface [24]. Since an identical Pt-coated counter electrode was employed for all DSSCs, the influence of Z_1 may be ignored. Therefore, the main emphasis of this study is on the impedance Z_2 relating to electron transfer at the TiO_2/dye/electrolyte interface. The parameters of R_2 (the real part of Z_2), which represents the interfacial recombination resistance, were fitted to the equivalent circuit inset in Fig. 6 and are summarized in Table 1. It is obvious that R_2 of DSSCs with Ag–TiO_2 composite photoanodes apparently increases with increasing Ag–NP additions. The larger the R_2, the less the dark current generated from charge recombination with triiodide ion and excited dye at the TiO_2/dye/electrolyte interface [21,25], and thus the larger the J_{sc}. This demonstrates that Ag–NPs as electron–hole separation centers due to Schottky barriers at the Ag/TiO_2 interface successfully reduce charge recombination reaction between electrons emanating from TiO_2 network and I_3^- present in the electrolyte [19].

Fig. 7(a) shows V_{oc} decay characteristics of the DSSCs with different Ag–NP content. The rate of the voltage attenuation can reflect the lifetime of the electrons to some extent. It was noted that the V_{oc} of the devices with Ag–NPs decayed more slowly than that of DSSCs with a pure TiO_2 photoanode, which implies a longer electron lifetime than that of pure TiO_2 DSSCs [26]. The electron lifetime shows an increasing–decreasing trend, with the longest lifetime at 0.15 wt% Ag–NP loading, in good agreement with the J–V curves shown in Fig. 4(a). Fig. 7(b) shows the dark current–voltage characteristics of the DSSCs. The value of the dark current, to some extent, reflects the recombination level of electrons in the conduction band of TiO_2 with triiodide (I_3^-). The dark current of the DSSCs significantly decreased for the sample with 0.15 wt% Ag content, which can be attributed to the suppression of the recombination between triiodide (I_3^-) and electrons in the TiO_2 network. This noticeable variation in dark current is consistent with

Table 1
Photovoltaic properties of DSSCs as a function of Ag–NP loading.

Photoanodes	J_{sc}(mA cm^{-2})	V_{oc}(mV)	FF	η(%)	R_2(Ω)
TiO_2	7.86	645	0.69	3.96	13.23
0.05 wt% Ag–TiO_2	8.92	653	0.67	4.42	14.11
0.10 wt% Ag–TiO_2	9.30	671	0.65	4.52	14.87
0.15 wt% Ag–TiO_2	10.19	698	0.67	5.33	15.78
0.20 wt% Ag–TiO_2	8.23	686	0.66	4.10	17.69

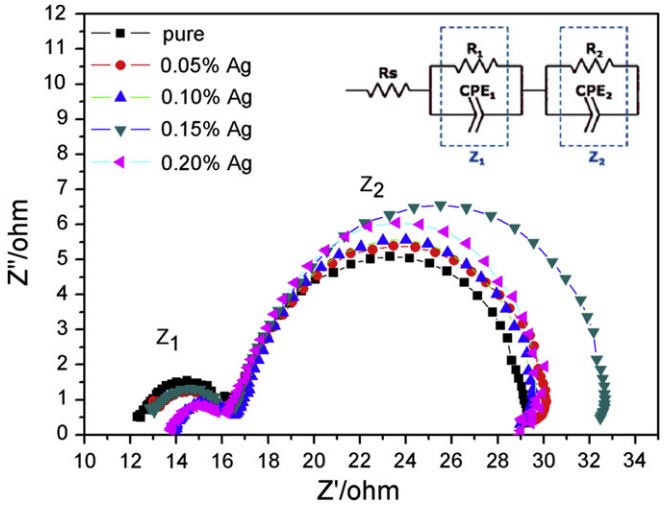

Fig. 6. EIS spectra of Ag–NPs modified DSSCs as a function of loading.

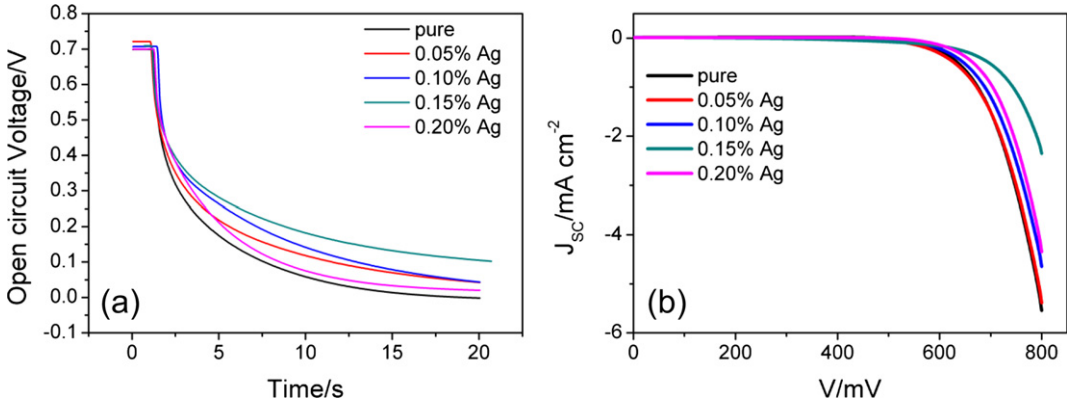

Fig. 7. V_{oc} decay (a) and dark current characteristics (b) as a function of loading for Ag–NPs modified DSSCs.

the J–V curves of the DSSCs, and would also make a contribution to increasing the V_{oc} of DSSCs.

4. Conclusions

A series of TiO_2 photoanodes with differing amounts of Ag–NPs in Ag@TiO_2 core–shell form were prepared and applied to make a series of DSSCs. The influence of Ag–NPs on the structure and performance of Ag–TiO_2 composite photoanodes and DSSCs was investigated. The results demonstrated that adding Ag–NPs to TiO_2 photoanodes significantly improved the performance of the DSSCs by increasing short-circuit current and open-circuit voltage, reducing dark current and prolonging electron lifetime. The best performing DSSC contained 0.15 wt% of Ag–NPs, and gave a J_{sc} of 10.19 mA cm^{-2}, a V_{oc} of 698 mV and a photoelectric conversion efficiency η of 5.33%, greatly superior to those of DSSCs using pure TiO_2 photoanodes. The increase of J_{sc} is attributed to the enhanced light absorption and broadened absorption spectral range of the composite photoanode due to the SPR of the Ag–NPs, While the V_{oc} increase may be reasonably related to the more negative quasi-Fermi energy of the Ag–TiO_2 composite system due to the enhanced electron capture and storage capability resulting from Ag–NP doping.

Acknowledgements

This work was supported by the National Basic Research Program of China (granted No. 2011CB933304) and the Fundamental Research Funds for the Central Universities (Granted No.: 20102020101000036).

References

[1] B. O'Gegan, M. Grätzel, Nature 353 (1991) 733–739.
[2] M.K. Nazeeruddin, R. Humphry-Baker, P. Liska, M. Grätzel, J. Phys. Chem. B 107 (2003) 8981–8987.
[3] P. Guo, M.A. Aegerter, Thin Solid Films 351 (1999) 290.
[4] S. Chappel, A. Zaban, Sol. Energy Mater. Sol. Cells 71 (2002) 141.
[5] K. Keis, C. Bauer, G. Boschloo, A. Hagfeldt, K. Westermark, H. Rensmo, H. Siegbahn, J. Photochem. Photobiol. Chem. 148 (2002) 57.
[6] M. Gräzel, J. Photochem. Photobiol. 4 (2003) 145.
[7] T.H. Meen, W. Water, W.R. Chen, S.M. Chao, L.W. Ji, C.J. Huang, J. Phys. Chem. Solids 70 (2009) 472.
[8] L.H. Hu, S.Y. Dai, J. Weng, S.F. Xiao, Y.F. Sui, Y. Huang, S.H. Chen, F.T. Kong, X. Pan, L.Y. Liang, K.J. Wang, J. Phys. Chem. B 111 (2007) 358.
[9] M. Adachi, Y. Murata, J.-T. Kao, J.-T. Jiu, M. Sakamoto, F.-M. Wang, J. Am. Chem. Soc. 126 (2004) 14943.
[10] G.K. Mor, K. Shankar, M. Paulose, O.K. Varghese, C.A. Grimes, Nano Lett. 6 (2006) 215.
[11] X.J. Feng, K. Shankar, O.K. Varghese, M. Paulose, T.J. Latempa, C.A. Grimes, Nano Lett. 8 (2008) 3781.
[12] M. Durr, S. Rosselli, A. Yasuda, and G. Nelles, J. Phys. Chem. B, 110 (51) 26507.
[13] E. Palomares, J.N. Clifford, S.A. Haque, T. Lutz, J.R. Durrant, J. Am. Ceram. Soc. 125 (2) (2003) 475–482.
[14] X.L. Fang, M.Y. Li, K.M. Guo, Y.D. Zhu, Z.Q. Hu, X.L. Liu, B.L. Chen, X.Z. Zhao, Electrochim. Acta 65 (2012) 174–178.
[15] Y.S. Kang, S. Risbud, J.F. Rabolt, P. Stroeve, Chem. Mater. 8 (1996) 2209–2211.
[16] C.P. Collier, R.J. Saykally, J.J. Shiang, S.E.H.J.R. Henrichs, Science 277 (1997) 1978–1981.
[17] M. Ihara, K. Tanaka, K. Sakaki, I. Honma, K. Yamada, J. Phys. Chem. B 101 (26) (1997) 5153–5157.
[18] K.L. Kelly, E. Coronado, L.L. Zhao, G.C. Schatz, J. Phys. Chem. B 107 (30) (2003) 668–677.
[19] J. Herrmann, J. Disdier, P. Pichat, J. Phys. Chem. 90 (1986) 6028–6034.
[20] C. Hägglund, M. Zäch, B. Kasemo, Appl. Phys. Lett. 92 (2008) 13113.
[21] C. Harris, P.V. Kamat, ACS Nano 4 (2010) 7321–7330.
[22] A. Takai, P.V. Kamat, ACS Nano 5 (2010) 7369–7376.
[23] G.L. Zhao, H. Kozuka, T. Yoko, Sol. Energy Mater. Sol. Cells 46 (1997) 219.
[24] L. Han, N. Koide, Y. Chiba, T. Mitate, Appl. Phys. Lett. 84 (2004) 2433.
[25] C.S. Chou, R.Y. Yang, C.K. Yeh, Y.J. Lin, Powder Technol. 194 (2009) 95–105.
[26] A. Zaban, M. Greenshtein, J. Bisquert, ChemPhysChem 4 (2003) 859–864.